International Journal of Recent Technology and Engineering (IJRTE)
ISSN: 2277-3878 (Online), Volume-7, Issue-6, March 2019

A MIMO-OFDM Based Secure and Robust Communication System for IOT Driven Healthcare

Uzma, Ghulam M. Bhat, Javaid A. Sheikh

Abstract: ***E-health is a comprehensive term applied for the joint utilization of communication technologies with electronic information for health sector. Internet of Things (IoT) in conjunction with Cyber Physical systems (CPS) is an emerging paradigm that is supposed to hugely influence e-health services round the globe. One of the core issues that need to be addressed in an IoT driven e-healthcare system is the security and robust transmission of Electronic Health Record (EHR) in a fading channel environment. For reliable and high speed transmission of critical electronic information, we have exploited Multiple Input Multiple Output, Orthogonal Frequency Division Multiplexing MIMO-OFDM technology. This paper presents a secure and robust technique for transmission of medical images with EHR hidden in them for an IoT driven e-health setup. The Orthogonal Variable Spreading Factor (OVSF) codes have been put to use for robustness enhancement of critical medical information during its transmission. In order to upturn the reliability of the transmission link and hence the robustness of the developed system, the antenna diversity order has been exploited. To ensure security of EHR, information hiding has been used to embed EHR in cover medical images prior to its transmission. Spatial domain embedding techniques, Least Significant Bit (LSB) and Intermediate Significant Bit (ISB) substitution, due to their lesser computational complexity have been used for Electronic Patient Record (EPR) embedding. The proposed scheme has been evaluated in terms of various image quality indices. The results obtained show that the proposed scheme is capable of transmitting EPR securely and robustly. A comparison of the proposed scheme with some state of art techniques shows that our system performs better in a real fading environment.***

Index Terms**: *Cyber Physical Systems, Embedding, Internet of Things, Robustness, Security, Watermarking.***

I. INTRODUCTION

The ease to internet access has revolutionized the world around. With people getting more and more tech-savvy, various things of everyday life have changed from their conventional nature to e-based commodities. The things like e-commerce, e-shopping, e-banking, e-education, e-healthcare and many more have surfaced. "Electronic healthcare refers to an internet based system wherein a patient can avail the services of an expert doctor available at other corner of globe" [1]. The key objective of e-healthcare is to help patients, doctors and community health centres to make optimum use of Information and Communication Technologies (ICTs) with an aim to improve the access and quality of healthcare delivery at reduced costs of its management [2]. The e-healthcare system has been a boon to the mankind in various ways, it has made the management of health records easy, diagnosis more accurate and at the same time it has reduced the need for the repeated tests while visiting different doctors. From computing point of view e-healthcare systems should be fast and highly reliable, as the decision making has to be done in the real-time. Thus cluster computing could be used in such a scenario. In cluster computing, computational powers of various nodes connected in the cluster are joined in such a way to provide combined and hence better computational power. Now-a-days a lot of research effort is being put in the area of IoT and CPS driven e-health care systems. Internet of Things (IoT) is a network of physical objects to enable communication and sensing within their internal states or the external environment. The emergence of various computing paradigms like cluster computing, parallel and distributed computing; convergence of resourceful wireless protocols, better-quality sensors, and cheaper processors is a driving factor for an IoT based healthcare setup [3-7]. Further, Cyber-Physical systems (CPS) represent networked assemblies of interacting devices, sensors, and hardware and software services for collaboratively realizing new functions. CPS are often large-scale systems that are supposed to monitor and control physical as well as organizational and business processes in real-time require a high degree of autonomy. The design of CPS and the implementation of their applications need to rely on IoT-enabled architectures and protocols that facilitate collecting, managing and processing large data sets, and support complex. In a typical IoT driven e-health setup, different wearable devices are used and interconnected by a wireless communication set up. Thus a lot of inter-device communication takes place so as to arrive at proper patient diagnosis. For successful implementation of an IoT driven e-healthcare system, two fields viz. biomedical image processing and communication form a pivotal part. While lot of work has been done on the part of biomedical image processing, an exhaustive research survey reveals that relatively less work has been done in the area of robust EHR communication.

Revised Manuscript Received on 30 March 2019.
***** Correspondence Author
Uzma, PG Deptt. Of Electronics and IT, University of Kashmir, Hazratbal, Srinagar, India.
Ghulam M. Bhat, Institute of Tecnology, Zakura Campus.University of Kashmir, Srinagar, India.
Javaid A. Sheikh, PG Deptt. Of Electronics and IT, University of Kashmir, Hazratbal, Srinagar, India.

The work presented in this paper is an attempt to develop a robust communication system utilizing the current generation communication techniques for transfer of EHR in wireless fading environment. To achieve our goal

MIMO-OFDM technology has been used. MIMO-OFDM is the strong candidate for 4G LTE, specially, in Internet applications and cellular communication [8]. In OFDM, the data stream, to be transmitted, is divided into a number of smaller sub-streams which are transmitted using a set of sub-carriers. The subcarriers used, have the least separation in their frequency domain, which is needed to maintain the orthogonality of their time-domain waveforms. As a result, the available bandwidth is used very efficiently. Fig 1 shows the general schematic of the MIMO-OFDM system.

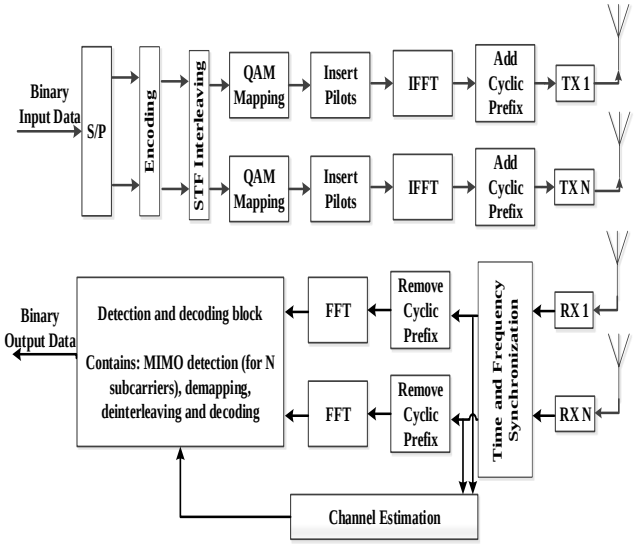

Fig 1: MIMO-OFDM System

OFDM has been appreciated as the most utilized signalling method in broadband wired [8] and wireless channels [9]. The use of more than one antenna at either ends of a wireless communication link is called Multiple-Input Multiple-Output (MIMO) technology [10]. It enhances the system's spectral efficiency and channel capacity at low power. Using multiple antennas basically creates number of spatial channels and the simultaneous fading of all the channels is improbable. In MIMO-OFDM system the data to be transmitted is first mapped into modulation symbols. An R×T matrix is formed through the serial to parallel conversion of R successive modulation symbols, where R and T represent the FFT size and the number of OFDM symbols in each slot, respectively. The corresponding rows of OFDM symbols can be space time encoded either using two successive symbols for Almouti's scheme or four successive symbols for the quasi orthogonal scheme, also for estimating the channel response a preamble is inserted at the start of each slot. The size of the preamble has to be as small as possible to avoid any serious reduction in transmission efficiency. For this one OFDM symbol is assigned for preamble and encoded in the frequency domain. MIMO systems may be implemented in different ways. They can be used to obtain either a diversity gain to combat signal fading, or to obtain a capacity gain [11]. The MIMO based wireless communication system uses Space Time Spread Coding Techniques for encoding and transmitting data into various paths so as to achieve diversity gain [10]. A number of space time spread coding techniques like beam forming, smart antennas etc., and have been proposed by various researchers. In [12] comparison of various MIMO-OFDM systems, with and without using adaptive beamforming has been presented. The observed results show that the BER performance of the system is enhanced with adaptive beamforming. In [13] authors have worked on the Application of MIMO Smart Antennas into WiMAX-OFDM System in Real Fading IEEE Standardized Channels. Keeping in view the advantages offered by MIMO-OFDM with regard to robust transmission of data we have implemented a new OVSF based medical image transmission system using MIMO-OFDM. The performance has also been evaluated over a Rayleigh fading channel for different antenna configurations. The results obtained show that the proposed technique has a lot of scope in biomedical multimedia communication. The paper provides the complete design of MIMO-OFDM system for secure and robust transmission of EHR in an IoT driven e-health setup. To ensure the orthogonality among OFDM carriers OVSF codes have been used. The work/design has been made adaptive in nature as different modulation schemes can be used for modulating the medical data for better reliability. For secure EHR transmission information hiding technology has been used. Further the link reliability has been enhanced for robust EHR transmission due the use of multiple links.Rest of the paper is organized as follows: Section II presents related work. Preliminaries required to understand the work have been elaborated in detail in Section III. Section IV gives description and implementation of proposed scheme. The performance metrics and experimental results have been discussed in Section V and Section VI respectively. The paper concludes in Section VII.

II. RELATED WORK

Owing to the exponential development of technologies and wireless communication systems there has been a rapid growth in electronic health care system development, for providing effective services to the community. The prominent areas of work reported so far include, data and EPR embedding in medical images, encryption of medical images and design of reversible data embedding systems for medical images [14-17]. However, to our best of knowledge no substantial research in the robust transmission of medical images/EHR over fading channels has been reported so far. A brief survey of literature has been presented below which lays a basis of the present research paper:Chemak et.al in [18] have explained a novel watermarking system for the protection of medical information and its adjustment with the terminal mobile phone (doctor's phone) for pocketneuro project. The term pocketneuro refers to a project formed for the examination of neurological diseases. The objective of the project had been to transmit the information regarding the patient to the doctor's mobile phone, when doctor is examining his patient. The system under consideration in the project is able to embed medical information inside the medical image for the security purposes. The authors have presented a robustness image watermarking scheme.

The scheme has been shown to be robust towards JPEG compression and capable of embedding large data payloads, all while maintaining the fidelity of images.

The scheme discussed embeds information in the multi-resolution field. Turbo codes which belong to the class of error correcting codes have been used to code the embedded information. Relative Peak Signal-to- Noise Ratio (RPSNR) has been used to estimate image deterioration after watermarking process to enhance the visual fidelity. A robust scheme for medical data transmission has been reported in [19]. In the reported work spatial domain watermarking has been used to embed the patient information as a watermark into the least significant bit of the medical image to reduce the storage and transmission overheads. The watermark consisting of some selected text has been encrypted to avert unauthorized access of data. In addition to this the encrypted watermark is coded by combination of Reed Solomon (RS) and low density parity check (LPDC) codes, to improve the stoutness of the embedded data. The watermarked image has been transmitted over fading channels. The performance reported has been evaluated in terms of channel capacity and objective parameters like Signal to Noise Ratio (SNR) and BER. An image transmission system utilizing OFDM with different modulation techniques through AWGN channel has been reported in [20]. It has been reported that quality of the recovered image is better at reasonably high SNR values irrespective of the modulation technique used. At low SNR, the quality of the recovered image is not up to mark due to the presence of high amount of AWGN noise. It has been found that the OFDM system with 16-QAM modulation technique provides less number of errors and high quality of the recovered image at the receiver compared to OFDM system implemented with other modulation techniques like M-PSK and M-QAM. For proper tele-diagnosis, reversible and high capacity data hiding system using Pixel Repetition technique (PRT), has been reported in [21]. The system proposed is capable of any sort of tamper detection. For this purpose a fragile watermark, computed from checksum of the cover medium blocks has been embedded in addition to EPR. Block-wise division of cover image and Intermediate Significant Bit (ISB) substitution have been used for data embedding. Transmission of polar coded grayscale images over AWGN channels using OFDM modulation scheme has been reported in [22]. The performance of the said channel has been evaluated by transmitting still images through the 64-QAM modulated OFDM system using polar codes. The comparison of polar codes with Bose–Chaudhuri–Hocquenghem (BCH) codes is performed in the same scenario. The investigated results show that the performance of the polar codes is much better than the performance of BCH codes in terms of perceptual quality of received images and the bit error probability. A digital watermarking scheme for medical images has been presented in [23]. To reduce the storage and transmission overhead the patient information has been embedded in medical image. Greater security has been ensured by encrypting the hidden patient data before embedding it in cover medical image .The graphical signals have been interleaved with the image. For transmission reliability and medical image storage, two types of coding techniques have been used. Transmission and storage scenarios have been simulated with and without error control coding. The qualitative as well as quantitative interpretation of the reliability enhancement, resulting from the use of various commonly used error control codes has been analysed and presented. Authors in [24] have proposed a high capacity and reversible data hiding technique that is capable of detecting any sort of temper and image localization. The original medical image has been scaled up, to obtain the cover medical image using image interpolation. In order to facilitate the reversibility of the proposed algorithm the EPR has been embedded only in the non-seed pixels and no embedding has been done on seed pixels. In addition to EPR, a fragile watermark coupled with Block Checksum has been embedded for temper detection of patient data during its transmission from transmitter to receiver. ISB substitution has been in this work for embedding to prevent the algorithm from LSB removal/replacement attack. The proposed scheme has been assessed for perceptual imperceptibility and content authentication by subjecting the proposed algorithm to various image processing and geometric attacks. A comparison of the observed results with some state-of-art schemes show that the reported scheme performs better and as such can be considered as an ideal candidate for content authentication of EPR in a typical e-healthcare system. In [25], a blind watermarking technique has been reported for tamper detection of medical images. The watermark has been formed by combining the patient information and arithmetic mean of Region of Interest (ROI) part of the image. The payload reported in the paper is 35,000 bits for a 512 × 512 pixel cover medical image. A histogram processing based, high capacity, block based and reversible watermarking algorithm has been proposed by authors in [26]. Loan et.al in [27] has presented a DCT based secure and blind watermarking scheme. Watermark has been secured by utilizing Arnold transform and chaotic encryption. The host image is divided into 8 × 8 non-overlapping blocks prior to DCT application, and the watermark bit is embedded by modifying difference between DCT coefficients of adjacent blocks. Authors claim that the proposed algorithm performs better in terms of robustness, security, and imperceptivity. Given the merits of the proposed scheme, it can be used in applications like e-healthcare and telemedicine to robustly hide electronic health records in medical images. In [28], hybridization of compression and cryptography algorithms have been proposed for medical image watermarking for E-healthcare applications. In this work the ROI part is segmented separately using a region growing algorithm. The region is then encrypted using Secure Hash Algorithm-256 and encrypt the electronic health record (EHR) using the elliptical curve cryptography algorithm. The information is then compressed using an arithmetic coding algorithm. The compressed bits are embedded into the original image. Most of the work carried out on EPR embedding in medical images deals with capacity, security, authentication and payload improvement without considering the EPR data transmission in fading environment.

In contrast to above mentioned work, this paper presents the practical scenario for the transmission of watermarked medical images in a real fading environment. This paper proposes a MIMO-OFDM based technique to improve the reliability and robustness of the watermarked medical image transmission over the fading channels. MIMO-OFDM system has been exploited for its diversity and link reliability is guaranteed by the presence of multiple links at both ends of the transmission link. In addition to this OVSF codes have been used. These codes have the added advantage of maintaining orthogonality between different channels in a communication system. The proposed scheme has been seen to be capable of successful reception of the watermarked medical image after taking all the transmission losses into account. The transmission has been tested on a number of digital modulation schemes of the 4G LTE which makes the work more adaptive in nature.

III. PRELIMINARIES

This section presents various preliminaries required to understand and fully appreciate the work done in this paper:

A. Watermarking

Watermarking has been developed from the oldest field of Steganography, which deals with the hiding of data [29-30] within some other sources for secure communication. Watermarking differs from the conventional steganography in its utilization. In steganography main motive is the capacity, up to which, data could be hidden in the cover image (host image) while as watermarking is mainly used for copyright protection, copy protection and authentication. The escalating amount of applications using digital multimedia technologies has accentuated the need to endow the copyright protection to multimedia data [31] and in this sense the field of watermark has a long way to go. Watermarking is usually described by various attributes, of which the most important are: 1) Embedding effectiveness which describes watermark(s) detecting probability, usually at the receiving point. 2) Perceptual similarity which defines the similarity between the original and watermarked image. 3) Robustness is the measure of the degree with which the watermarked image can withstand different attacks and various image processing operations like compression, filtering and geometric distortion. 4) Data embedding capacity which refers to the number of bits that could be embedded within a cover (host image). There are various methods of watermarking of which Least Significant Bit (LSB) substitution is easy to implement.

B. Least Significant Bit Substitution Watermarking

LSB algorithm is very simple, effective and computationally least complex, thus making it a candidate for real time information embedding applications [32]. The watermark embedding is carried out by selecting a subset of image pixels and substituting the least significant bit of each of the selected pixels with watermark bits. For further understanding of the concept readers are kindly referred to [33-34]. Fig 2 shows the railway track image and corresponding watermarked image obtained by embedding message "HELLO" in the cover image by LSB embedding. The watermark extraction is performed by extracting the least significant bit (LSB) of each of the chosen image pixels. If there is a match between the extracted bits and the inserted bits, then the watermark is detected.

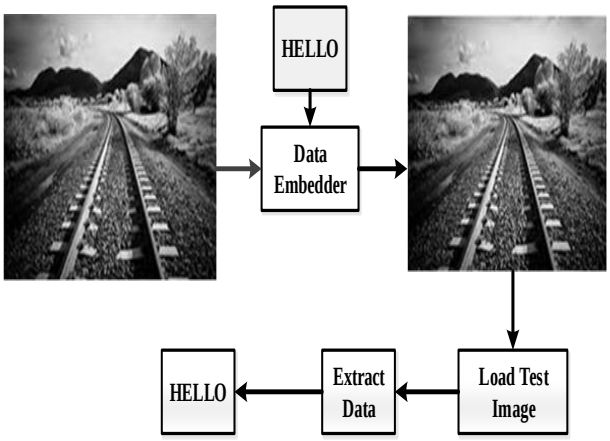

Fig 2: Schematic of Least Significant Bit Substitution

C. Intermediate Significant Bit Substitution Watermarking

Although LSB algorithm is very easy to implement but LSB is extremely vulnerable to corruption. To avoid such a loss the watermark is embedded in bits other than LSB of the original image. In the 8-bit representation of grey-scale images, the first bit-plane contains the set of the most significant bits, while the 8th bit-plane contains the least significant bits, and the set in between, from the 2nd to the 7th bit-planes, are intermediate significant bits (ISB) [14]. When the ISBs of the host image are replaced with the watermark bits it is called as ISB watermarking. Accordingly it can be 1st ISB, 2nd ISB and so on.

IV. PROPOSED WORK

The proposed system has been discussed in detail in this section. The complete schematic of the proposed system has been presented in Fig 3. Various subsystems of the proposed system have been presented as follows:

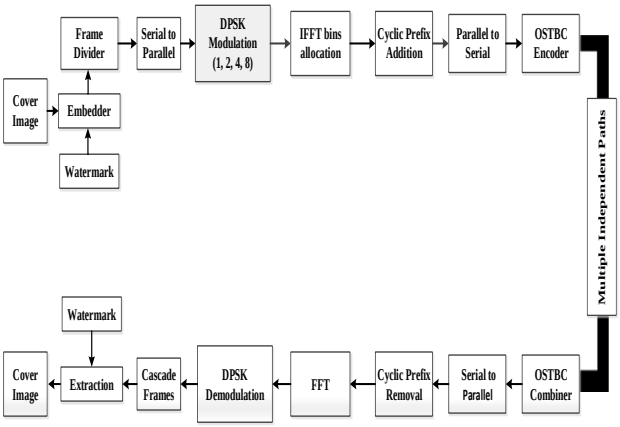

Fig 3: Schematic of the proposed system.

A. OFDM Transmitter

The medical image to be transmitted is embedded with medical data using LSB technique. LSB has been discussed in detail in section 3.2.The data is then encoded using OVSF coding. The core of the OFDM transmitter is the modulator, which modulates the input data stream frame by frame. Data is divided into frames with each frame referring to the number of symbols per carrier. Usually the total number of transmitted data symbols is not a multiple of the number of carriers. For the data to fit into the 2-D matrix the modulator pads the data at its end, for its serial to parallel conversion. The data, as per the PSK order chosen by the user, is arranged into the corresponding symbol size. This is the desired baseband signal for OFDM modulator which has been implemented by using Inverse Fast Fourier Transformer (IFFT). To avoid inter block interference among various blocks of data the cyclic prefix is added at the start of each block. For this 12.5 % symbols of each block are prefixed at the start of each block. For transmission the data is then concatenated along with their headers and tailors. For MIMO transmission the data is fed to Orthogonal Space Time Block Encoder (OSTBC), which encodes the data using orthogonal space time block code. This encoder maps the input symbols block-wise and provides the concatenated output code-word matrices in the time domain [35]. The various plots obtained at the simulated transmitter are shown in Fig 4 below.

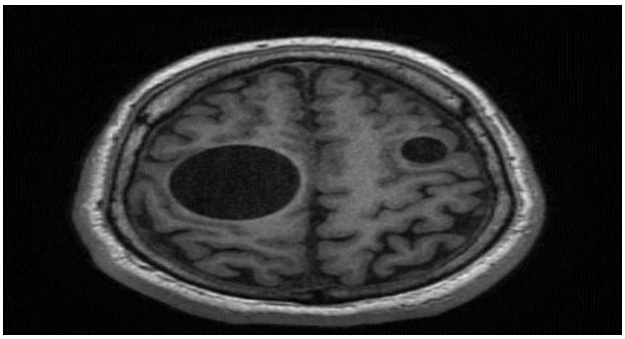

(a)

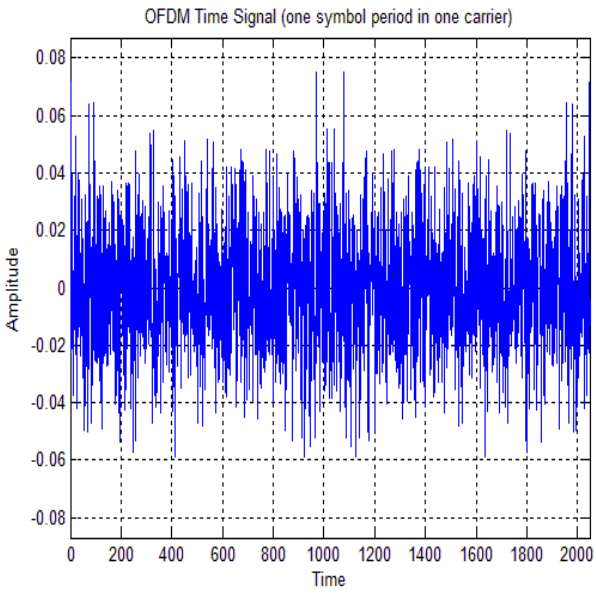

(b)

Fig 4: (a) Input Watermarked Image, (b) Waveform of OFDM Signal.

B. Channel

The data which includes image data with EPR embedded within it, is transmitted through independent Rayleigh channels created by the decomposition of MIMO channel matrix.

C. OFDM Receiver

At the receiving end the encoded data is fed to OSTBC combiner. The combiner combines the input data received from all the receiving antennas and channel estimates the signal to get the information of the symbols encoded by OSTBC encoder [35]. The start and end of each data frame is then detected using an envelope detector. 12.5% length of each symbol period is removed from all parallel streams of data. Each detected frame of the time signal is then demodulated into the useful data. The data is then decoded for OVSF coding. The decoded data is converted back to 8-bit word size data that is then used for generating an output file of the simulation. The watermark is then recovered from the received image. The performance of various modulation schemes with different SNR has been shown in Fig 5. It is pertinent to mention that the image shown in Fig 4(a) has been modulated using QPSK modulation, with 2048 IFFT size, and 1009 carriers and with 15 dB SNR. The phases of the data received have been shown in Fig 5(a). Since the data (image) is modulated using QPSK modulation scheme and QPSK uses four points on the constellation diagram that are equi-spaced around a circle. With these phases, QPSK can basically encode two bits per symbol. Thus QPSK modulation can either be used to double the data rates as compared to a BPSK modulation at the same bandwidth of the signal or it can be used to maintain the data rate of BPSK at a half bandwidth. The implementation of QPSK is more general than that of BPSK and also facilitates the implementation of higher order PSK. The BER plot of various modulation schemes viz BPSK, QPSK, 16-PSK and 256-PSK for the transmission of Img10 has been shown in Fig 5(b). The pixel error plot of these modulation schemes with increasing SNR (for Img10) has been presented in Fig 5(c). Likewise the PSNR for the same image obtained at different SNR for various digital modulation schemes has been shown in Fig 5(d).

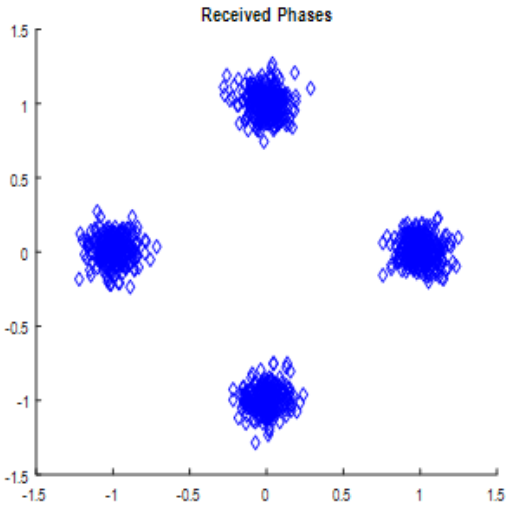

(a)

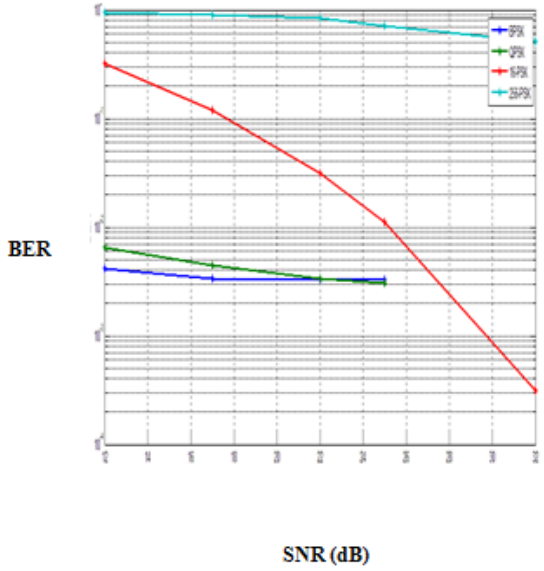

(b)

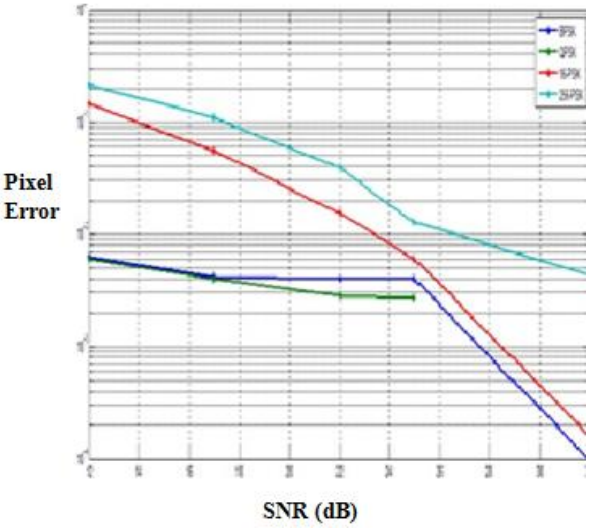

(c)

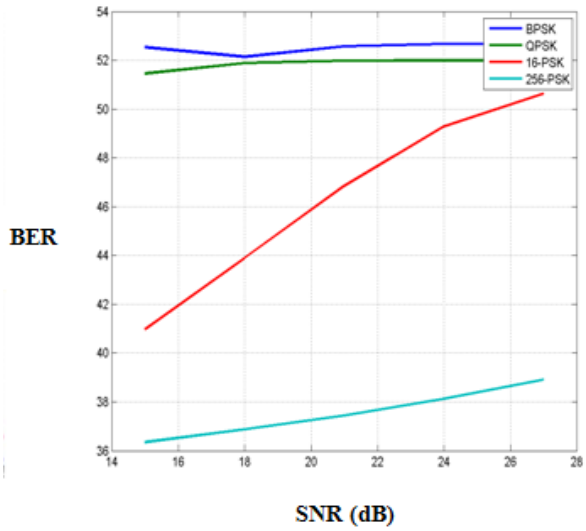

(d)

Fig 5: Receiver Plots of various modulation schemes (a) Received Phases of MIMO-OFDM Signal, (b) BER plot, (c) Pixel error plot, (d) PSNR plot.

The plot between SNR and BER (Fig 5b) clearly shows that with increase in SNR, the BER goes on decreasing for all the modulation schemes. The BER is least for BPSK however the bandwidth requirement is greater. QPSK has greater BER as compared to BPSK and the bandwidth required is comparatively less. We have chosen QPSK for this work as it provides a good trade-off between error rate and bandwidth. Phase error plot of the Img10 for various modulation schemes has been shown in Fig 5c. It is evident from the Fig 5c that as the SNR is increased; the received phases approach the respective transmitted phases. Fig 5d presents the variation in PSNR of the received image as a function of SNR for various modulation schemes. It is evident that as SNR at the transmitter is increased for a given antenna configuration; channel noise decreases gradually and leads to better reception at the receiver.

V. PERFORMANCE METRICS

The performance of the proposed scheme has been evaluated using following performance metrics.

A. Bit Error Rate (BER)

The total number of errors that has occurred during transmission are calculated by comparing the demodulated/received data to the original transmitted data. The bit-error-rate (BER) is calculated by dividing the total number of errors by total number of demodulated symbols.

$$\text{BER} = \frac{\text{num. of bits in error}}{\text{total no of bits transmitted}}$$

B. Pixel Error

The above mentioned performance metrics are related to the OFDM symbols but what seems to be more important to the system user is the actual error in the pixels of the received image. This error is obtained by comparing the received image and transmitted image pixel by pixel.

C. Peak Signal to Noise Ratio (PSNR)

PSNR is the ratio between maximum possible power and corrupting noise that affect the representation of image. PSNR is usually expressed in decibel scale [31]. High value of PSNR indicates the high quality of image. The recovered image after demodulation is checked for PSNR by comparing it with the original transmitted image.

$$PSNR = 20\log\left(\frac{max^2}{MSE}\right)$$

Where MSE is calculated as,

$$\text{MSE} = \frac{1}{XY}\sum_{i=0}^{1-X}\sum_{j=1}^{1-Y}[O(i,j) - W(i,j)]^2$$

Where X and Y are the number of rows and columns in the input images and O, W represent the original and watermarked images respectively.

D. Structural Similarity Index (SSIM)

The Structural Similarity Index (SSIM) is based on the calculations of three terms, namely the luminance, contrast and structure [16] .The overall index is given by

$$\text{SSIM}(x,y) = [I(x,y)]^{\alpha}.[C(x,y)]^{\beta}.[S(x,y)]^{\gamma}$$

Where,

$$[I(x,y)] = \frac{2\mu_x\mu_y + c_1}{\mu_x^2 + \mu_y^2 + c_1}$$

$$[C(x,y)] = \frac{2\sigma_x\sigma_y + c_2}{\sigma_x^2 + \sigma_y^2 + c_2}$$

$$[S(x,y)] = \frac{\sigma_{xy} + c_3}{\sigma_x\sigma_y + c_3}$$

Where μ_x,μ_y,σ_x,$\sigma_y$and σ_{xy} are the local means, standard deviations, and cross-covariance for images x, y..

E. Normalized Cross Correlation (NCC)

This parameter is used to indicate the degree of similarity between the original image the deteriorated image. NCC between embedded watermark and recovered watermark is defined as

$$\text{NCC} = \frac{\sum_{i=1}^{M}\sum_{j=1}^{N} w_{OW}(i,j)w_{EM}(i,j)}{\sum_{i=1}^{M}\sum_{j=1}^{N} w_{OW}(i,j)^2}$$

Where $w_{OW}(i,j)$ is the (i,j)th pixel of the original watermark and $w_{EM}(i,j)$ is the (i,j)th pixel of the recovered watermark. As the correlation between the two images increases, the value of NCC approaches unity.

VI. EXPERIMENTAL RESULTS

The proposed scheme has been implemented using MATLAB 7.0 running on windows platform. The scheme has been evaluated for imperceptivity and robustness for the fading environment. We have used ten most commonly used medical images to test our algorithm. The size of the test image chosen is 512×512. The scheme has been evaluated in terms of subjective and objective quality metrics like PSNR SSIM, NCC and BER. Fig 6 shows various test images used to analyze the proposed scheme.

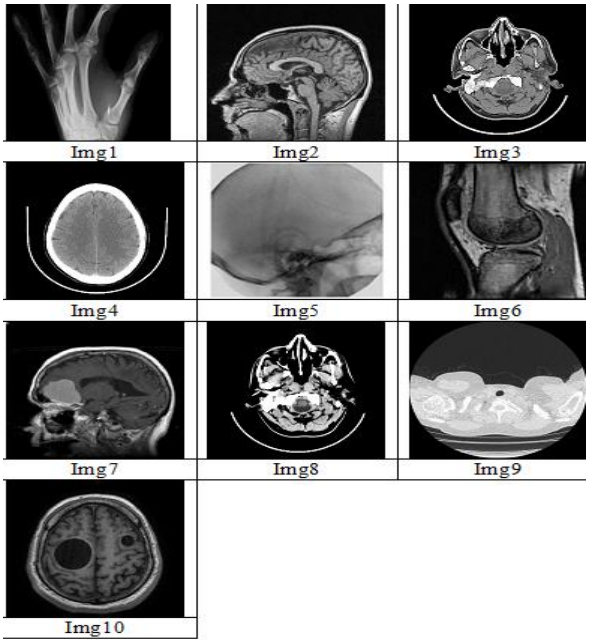

Fig 6: Host medical images (512×512) used to test the proposed transmission schemes.

A. Imperceptibility Analysis

We have embedded a payload of 2, 62,144 bits (1 bit per pixel) using simple LSB, 1st ISB and 2nd ISB substitution. It has been seen that the watermarked medical image is more degraded as we embedded data in higher order bit planes.

Fig 7 above shows the subjective quality of all the ten watermarked medical images when data has been embedded in 2nd ISB plane. The average PSNR prior to transmission has been found to be 50.6124 dB, 44.0278 dB and 38.0383 dB respectively for embedding a payload of 1 bit per pixel in LSB, 1st ISB and 2nd ISB planes.

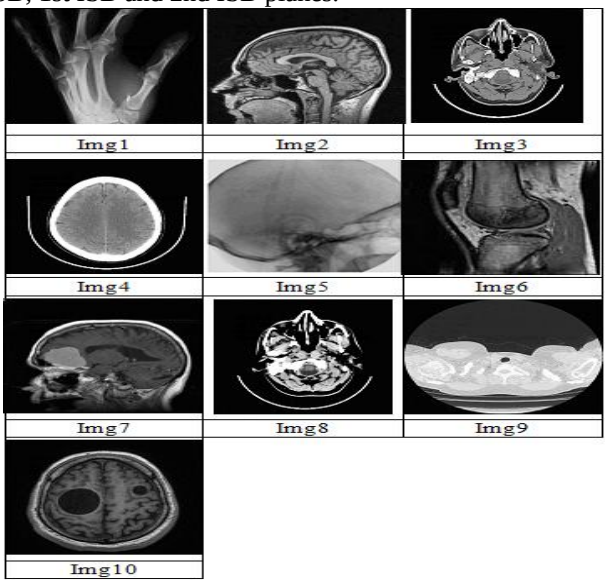

Fig 7: Watermarked medical images (512×512) used to test the proposed transmission schemes.

Various objective quality metrics (NCC and SSIM) of watermarked images for a payload of 262144 bits with different antenna configurations have been shown in Table 2 and Table 3.

The observed values show that our technique is capable of providing high quality watermarked images even for a very high payload. It is in place to mention here that embedding data in 1st and 2nd ISB guarantees the robustness of our scheme to commonly used LSB removal attack. We have compared the parameters obtained in our scheme to some existing state of art schemes like [24-26, 16]. The comparison results have been shown in Table 1.It is evident from the Table 1 that our scheme outperforms the techniques under comparison. The most important feature of our scheme being high PSNR for a relatively high payload compared to techniques under comparison.

Table 1: Comparison of proposed techniques with [24-26, 16].

Image	Scheme	Capacity (bits)	PSNR (dB)
Img2	Proposed	2,62,144	51.408
	[24]	1,96,608	46.476
	[26]	800	52.200
Img3	Proposed	2,62,144	49.056
	[24]	1,96,608	46.760
Img5	Proposed	2,62,144	51.192
	[16]	1,96,608	46.369
Img6	Proposed	2,62,144	51.148
	[16]	1,96,608	46.360
Img9	Proposed	2,62,144	50.352
	[24]	1,96,608	46.465
	[25]	35,000	56.588

We have evaluated our scheme for NCC and SSIM and the results have been presented in Table 2 and Table 3.

Table 2: SSIM and NCC calculation for different images for 2×1 antenna configurations with LSB substitution and QPSK modulation.

Image	SSIM			NCC		
	SNR 20	SNR 25	SNR 30	SNR 20	SNR 25	SNR 30
Img1	0.9431	0.9431	0.9431	0.9901	0.9945	1.0000
Img2	0.9980	0.9980	0.9980	0.9816	0.9904	1.0000
Img3	0.9182	0.9182	0.9182	0.9859	0.9932	1.0000
Img4	0.9220	0.9220	0.9220	0.9905	0.9932	1.0000
Img5	0.9967	0.9967	0.9967	0.9904	0.9933	1.0000
Img6	0.9962	0.9962	0.9962	0.9857	0.9904	1.0000
Img7	0.9639	0.9639	0.9639	0.9761	0.9939	1.0000
Img8	0.9120	0.9120	0.9120	0.9856	0.9926	1.0000
Img9	0.9731	0.9731	0.9731	0.9852	0.9903	1.0000
Img10	0.9730	0.9730	0.9730	0.9721	0.9931	1.0000
Avg.	0.9596	0.9596	0.9596	0.9843	0.9925	1.0000

Table 3: SSIM and NCC calculation for different images for 2×2 antenna configuration with LSB substitution and QPSK modulation.

Image	SSIM			NCC		
	SNR 5	SNR 10	SNR 15	SNR 5	SNR 10	SNR 15
Img1	0.9434	0.9434	0.9434	0.9800	0.9899	1.0000
Img2	0.9979	0.9979	0.9979	0.9820	0.9889	1.0000
Img3	0.9196	0.9196	0.9196	0.9859	0.9880	1.0000
Img4	0.9233	0.9233	0.9233	0.9803	0.9890	1.0000
Img5	0.9967	0.9967	0.9967	0.9800	0.9889	1.0000
Img6	0.9962	0.9962	0.9962	0.9871	0.9898	1.0000
Img7	0.9643	0.9643	0.9643	0.9759	0.9889	1.0000
Img8	0.9134	0.9134	0.9134	0.9850	0.9890	1.0000
Img9	0.9731	0.9731	0.9731	0.9851	0.9891	1.0000
Img10	0.9730	0.9730	0.9730	0.9709	0.9880	1.0000
Avg.	0.960 09	0.9600 9	0.9600	0.9812 2	0.9889 5	1.0000

A detailed analysis of the results depicted in Table 2 and Table 3 show that an increase in the power level for a given antenna configuration improves NCC as a results of decrease in channel error. However, SSIM is independent of power and antenna configuration and is strictly a function of substitution technique.

B. Robustness Analysis

In this section we present detailed robustness analysis of our technique for various embedding schemes, antenna configuration while modulating the data using QPSK at different power. Accordingly following cases arise for the analysis.

Table 4: Various cases under study.

Case	Antenna configuration	Embedding scheme	Modulation technique
I.	2×1	LSB	QPSK
II.	2×2	LSB	QPSK
III.	2×1	1st ISB	QPSK
IV.	2×2	1st ISB	QPSK
V	2×1	2nd ISB	QPSK
VI.	2×2	2nd ISB	QPSK

i. Robustness analysis for LSB embedding, QPSK modulation and various antenna configuration

In this subsection we present robustness analysis of our scheme with LSB embedding using QPSK modulation over different antenna configurations. The results obtained for 2×1 antenna have been presented in Table 5, while as Table 6 shows various indices for 2×2 antenna configuration keeping modulation and embedding techniques same as those used in Table 5.

Table 5: For 2×1 Antenna Configuration with LSB Substitution (QPSK Modulation)

Input Image	PSNR	SNR=20dB			SNR=25dB			SNR=30dB		
		PSNR1	BER1 (%)	BER2 (%)	PSNR1	BER1 (%)	BER2 (%)	PSNR1	BER1 (%)	BER2 (%)
Img1	49.6345	41.4331	3.8132	1.1951	44.4592	1.4935	0.7614	49.6345	0	0
Img2	51.4081	39.7920	3.7941	1.2562	45.8433	1.4088	0.4829	50.4078	0	0
Img3	49.0568	43.4062	3.5160	1.3016	47.5161	1.4557	0.4349	49.0568	0	0
Img4	49.2423	43.4420	3.3047	1.2127	45.5212	1.4946	0.4349	49.2423	0	0
Img5	51.1925	40.4796	3.6919	1.3077	45.4938	1.4488	0.4333	49.1925	0	0
Img6	51.1480	40.9480	3.5522	1.1887	48.0058	1.2894	0.4269	51.0043	0	0
Img7	54.7638	39.4355	3.4367	1.1951	45.5360	1.5247	0.4066	50.2895	0	0
Img8	48.9277	38.9367	3.5732	1.2157	43.5125	1.4408	0.6138	48.9277	0	0
Img9	50.3977	41.1463	3.7960	1.2211	47.2003	1.4675	0.4829	50.3977	0	0
Img10	50.3529	43.0190	3.5843	1.2493	47.0992	1.4652	0.4578	50.3529	0	0
Avg.	50.6124	41.2038	3.6062	1.2343	46.0187	1.4489	0.4935	49.8506	0	0

PSNR= Peak to Signal Ratio of Original Image w.r.t Watermarked Image.
PSNR1=PSNR of received Image w.r.t Transmitted Image at the Receiver.
BER1=BER of Received Image w.r.t Transmitted Image.
BER2=BER of Recovered Watermark w.r.t Embedded Watermark.

Table 6: For 2×2 Antenna Configuration with LSB substitution QPSK Modulation)

Input Image	PSNR	SNR=5dB			SNR=10dB			SNR=15dB		
		PSNR1	BER1 (%)	BER2 (%)	PSNR1	BER1 (%)	BER2 (%)	PSNR1	BER1 (%)	BER2 (%)
Img1	49.6345	27.5780	4.6518	0.9533	31.9260	1.2211	0.6168	49.6345	0	0
Img2	51.4081	27.8374	4.7876	0.9521	32.2502	1.3668	0.6031	51.4078	0	0
Img3	49.0568	28.0551	4.2562	0.9472	33.3805	1.4034	0.6363	49.0568	0	0
Img4	49.2423	27.8455	4.4214	0.9331	33.6004	1.4931	0.6393	49.2423	0	0
Img5	51.1925	27.1429	4.5339	0.9575	32.4896	1.2806	0.6462	51.1925	0	0
Img6	51.1480	28.3337	4.2398	0.9418	32.3884	1.3977	0.6313	51.1748	0	0
Img7	54.7638	27.8731	4.2875	0.9315	33.6115	1.5015	0.6451	54.7635	0	0
Img8	48.9277	28.1644	4.1242	0.9468	33.3770	1.4034	0.6401	48.9277	0	0
Img9	50.3977	28.0148	4.2711	0.9571	32.6312	1.2913	0.5993	50.3977	0	0
Img10	50.3529	29.8586	4.2173	0.9441	32.0122	1.4606	0.6142	50.3529	0	0
Avg.	50.6124	28.0703	4.3790	0.9464	32.7667	1.3819	0.62717	50.6150	0	0

The results shown in Table 5 reveal that an increase in the power level enhances the PSNR and decreases the BER. It has been observed that at SNR of 30dB PSNR1 approaches PSNR for 2×1 antenna configuration. It has also been observed that by exploiting antenna diversity order the system robustness improves tremendously. This is evident from the fact that BER1 and BER2 approach zero for an SNR value of 15 dB only for a 2×2 antenna configuration, while as for 2×1 configuration the same values approach zero at an SNR of 30 dB.

Table 7: For 2×1 Antenna Configuration with 1st ISB Substitution (QPSK Modulation)

Input Image	PSNR	SNR=20dB			SNR=25dB			SNR=30dB		
		PSNR1	BER1 (%)	BER2 (%)	PSNR1	BER1 (%)	BER2 (%)	PSNR1	BER1 (%)	BER2 (%)
Img1	43.5644	27.1901	3.2993	1.1005	30.1961	1.4702	0.5142	43.5644	0	0
Img2	44.7411	27.9741	3.511	1.0773	30.9418	1.5087	0.5169	44.7409	0	0

Img3	43.0146	27.7623	3.2955	0.901	30.752	1.5781	0.5142	43.0146	0	0
Img4	43.2154	27.8225	3.5934	1.0792	30.6668	1.4507	0.4959	43.2154	0	0
Img5	45.2077	26.0609	3.4092	1.0517	30.9814	1.3851	0.5333	45.2077	0	0
Img6	44.8111	26.8417	3.2944	0.9571	30.2123	1.4179	0.507	44.8069	0	0
Img7	43.9101	26.3404	3.3875	1.0963	29.8072	1.4835	0.5024	43.9101	0	0
Img8	42.8505	27.4778	3.2654	0.9724	29.8586	1.403	0.5013	42.8505	0	0
Img9	44.534	27.4015	3.2677	1.0971	30.8088	1.4633	0.5062	44.534	0	0
Img10	44.4296	26.9322	3.1029	0.8617	30.2223	1.4912	0.5253	44.4296	0	0
Avg.	44.0278	27.1803	3.3426	1.0194	30.4447	1.46517	0.5116	44.0274	0	0

ii. Robustness analysis for 1st ISB embedding, QPSK modulation and various antenna configuration

This section discusses the robustness analysis when 1st ISB of the host medical image has been replaced with the EPR embedded as watermark. The PSNR has been calculated in this case prior to transmission and then effect of increasing power levels and changing antenna configuration has been evaluated. The PSNR prior to transmission is lesser then the PSNR obtained in the LSB substitution and as the power is changed from 20 to 30dB in case of 2×1 antenna configuration PSNR1 approaches the PSNR. For 2×2 antenna configuration PSNR1 approaches PSNR at SNR of 15dB only. The detailed values obtained at each power level for 2×1 antenna configuration is given in Table 7 and for 2×2 antenna in Table 8.

Table 8: For 2×2 Antenna Configuration with 1st ISB Substitution (QPSK modulation)

Input Image	**PSNR**	**SNR=5dB**			**SNR=10dB**			**SNR=15dB**		
		PSNR1	**BER1 (%)**	**BER2 (%)**	**PSNR1**	**BER1 (%)**	**BER2 (%)**	**PSNR1**	**BER1 (%)**	**BER2 (%)**
Img1	43.5644	27.8225	4.4771	4.6700	41.0118	1.4211	1.2001	43.5644	0	0
Img2	44.7411	26.3107	4.6907	4.8393	39.7671	1.4179	1.3725	44.7409	0	0
Img3	43.0146	26.3142	4.6331	5.3410	40.7493	1.4473	1.2066	43.0146	0	0
Img4	43.2154	27.2014	4.6331	5.2315	41.5839	1.3660	0.8831	43.2154	0	0
Img5	45.2077	29.8072	4.4010	4.6787	39.1389	1.3596	1.1711	45.2077	0	0
Img6	44.8111	27.6507	4.5358	5.2334	41.4585	1.3996	1.1856	44.8069	0	0
Img7	43.9101	25.6145	4.7445	5.0217	39.5414	1.3826	1.4206	43.9101	0	0
Img8	42.8505	27.8911	4.2902	5.2353	37.5622	1.3847	1.4687	42.8505	0	0
Img9	44.5340	26.3504	4.4767	4.9927	35.6679	1.4317	0.8541	44.5340	0	0
Img10	44.4296	26.3862	4.6903	4.9957	36.7930	1.4854	1.3245	44.4296	0	0
Avg.	44.0278	27.1348	4.5572	5.0239	39.3274	1.40959	1.2086	44.0274	0	0

Like in LSB embedding technique, in this embedding technique also the error is minimized to zero at 30dB SNR for 2×1 antenna configuration and 15dB for 2×1 antenna system. One can conclude that BER at the receiver is independent of the embedding technique used at the transmitter.

iii. Robustness analysis for 2nd ISB embedding, QPSK modulation and various antenna configuration

We have evaluated our scheme with EPR embedded in 2nd ISB of host medical image for various fading scenarios. The values of PSNR obtained before and after transmission have been presented in Table 9 and Table 10. The observed values of PSNR clearly indicate that increase in power levels increase PSNR1 to approach PSNR.

This is due to minimization in the channel noise. BER has also been seen to improve with increased power levels. Table 9 depicts that for 2×1 antenna configuration BER and BER1 approaches zero at an SNR of 30 dB while as SNR of 15dB is sufficient to reduce BER and BER1 to zero in case of 2×2 antenna configuration.

Table 9: For 2×1 Antenna Configuration with 2nd ISB Substitution (QPSK Modulation)

Input Image	PSNR	SNR=20dB			SNR=25dB			SNR=30dB		
		PSNR1	BER1 (%)	BER2 (%)	PSNR1	BER1 (%)	BER2 (%)	PSNR1	BER1 (%)	BER2 (%)
Img1	37.4924	27.1099	3.8132	0.9792	29.8496	1.4935	0.5436	37.4924	0	0
Img2	38.4072	27.3947	3.7941	1.0334	28.0331	1.4088	0.6329	38.4072	0	0
Img3	37.0024	27.5847	3.5160	1.0227	31.6816	1.4557	0.5520	37.0024	0	0
Img4	37.2117	27.6778	3.3047	0.9212	28.1703	1.4946	0.5920	37.2117	0	0
Img5	39.0298	27.8504	3.6919	1.0624	30.3725	1.4488	0.7248	39.0298	0	0
Img6	39.9024	29.4190	3.4078	0.9644	30.6106	1.4894	0.5489	39.9024	0	0
Img7	37.5923	25.7669	3.8181	1.1158	31.2159	1.5247	0.6748	37.5923	0	0
Img8	36.8271	27.3341	3.5732	1.1429	31.8990	1.4408	0.7221	36.8271	0	0
Img9	38.5193	26.6443	3.7960	1.0521	28.0531	1.4675	0.7473	38.5193	0	0
Img10	38.3984	27.5452	3.5843	1.1303	28.1133	1.4652	0.6310	38.3984	0	0
Avg.	38.0383	27.4327	3.6299	1.0424	29.7999	1.4689	0.6369	38.0383	0	0

Table 10: For 2×2 Antenna Configuration with 2nd ISB Substitution (QPSK Modulation)

Input Image	PSNR	SNR=5dB			SNR=10dB			SNR=15dB		
		PSNR1	BER1 (%)	BER2 (%)	PSNR1	BER1 (%)	BER2 (%)	PSNR1	BER 1(%)	BER 2 (%)
Img1	37.4924	27.4228	6.1237	9.6737	30.9870	1.5526	1.5358	37.4924	0	0
Img2	38.4072	28.9172	6.4529	9.2949	30.7945	1.5148	1.4923	38.4072	0	0
Img3	37.0024	26.1890	6.3629	9.7088	30.1255	1.4267	1.5736	37.0024	0	0
Img4	37.2117	26.1328	6.6223	9.1949	30.7645	1.5121	1.4324	37.2117	0	0
Img5	39.0298	28.8734	6.4510	9.4772	31.9034	1.3653	1.4874	39.0298	0	0
Img6	39.9024	28.5188	6.6708	9.5814	30.5438	1.5587	1.7475	39.9024	0	0
Img7	37.5923	26.4338	6.7505	10.4832	31.2578	1.4610	1.4629	37.5923	0	0
Img8	36.8271	25.6599	6.3850	9.5810	31.3229	1.5053	1.4290	36.8271	0	0
Img9	38.5193	28.1937	6.2667	9.3937	31.0000	1.5156	1.5564	38.5193	0	0
Img10	38.3984	28.0935	6.0154	9.8133	30.9237	1.5282	1.5465	38.3984	0	0
Average	38.0383	27.4435	6.4101	9.6202	30.9623	1.4940	1.5263	38.0383	0	0

The objective equality robustness analysis of different variants of our scheme has been presented in Tables 5 to 10. The scheme has been evaluated in terms of PSNR and BER. It has been seen that irrespective of embedding technique BER reduces with increase in power levels for a given antenna configuration. Further it has been observed that robustness of the proposed scheme increases with increase in antenna diversity order. An interesting observation worth noting is that for a given embedding scheme and SNR, performance enhances drastically as a function of increase in antenna diversity.

A. Robustness analysis of the system based on its subjective quality metrics

In this sub-section we present subjective quality based robustness analysis of our scheme. For This analysis we have arbitrarily chosen Img10. From subjective quality point of view, an algorithm is considered robust if we are able to extract the embedded watermark in a recognizable form. The analysis has been carried out for all the six cases mentioned in Table 4.

i. Subjective analysis for case I and II

Under this analysis the perceptual recognisability of the watermark at different power levels has been discussed. It is evident from Fig 8 and 9 that for 2×1 antenna diversity extracted watermark is completely visible (recognizable) for SNR of 30 dB, whereas when antenna diversity is 2×2 the received information is visible at 15dB only. This is in tune with the objective quality results as already reported in Table 5 and 6.

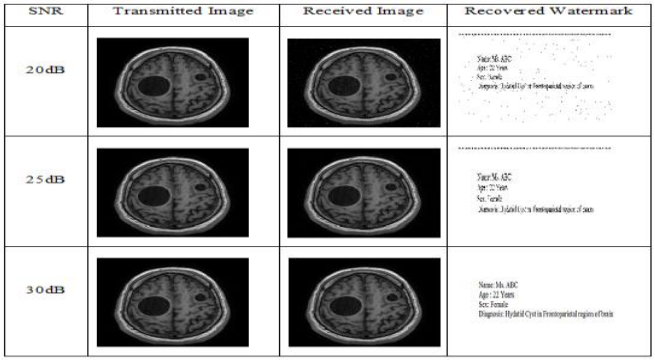

Fig 8: For 2×1 Antenna Configuration with LSB Substitution

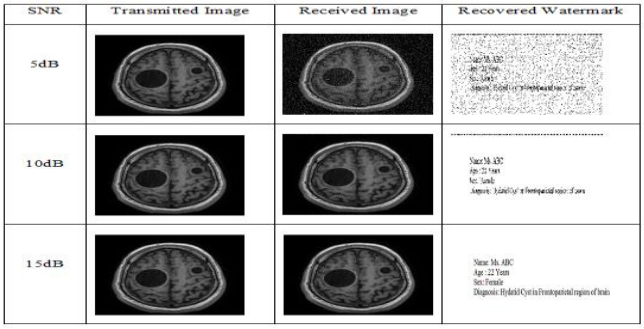

Fig 9: For 2×2 Antenna Configuration with LSB Substitution

From the Fig 8 and 9 the effect of noise on the recovered watermark over various antenna configurations at different power levels, which effects the readability of the watermark is clearly visible. The effect of noise on the recovered watermark are perceived in the form of various spots, that are visible from the watermark recovered at 20 dB and 5dB for 2x1 and 2x2 antenna configuration respectively. The watermark is clearly visible at the power levels where the BER1 and BER2 are both zero.

ii. Subjective analysis for case III and IV

The subjective quality images obtained for 1st ISB substitution have been shown in Fig. 10 and Fig. 11. Like in above mentioned cases (I and II) the two cases under discussion (III and IV) also follow the same trend. As the antenna configuration is changed from 2×1 to 2×2 the received information is completely readable at lower values of SNR. Again one finds that the results are in sync with the results presented in Table 7 and 8.

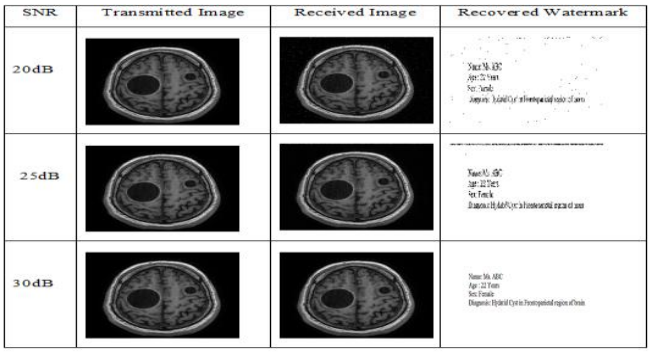

Fig 10: For 2×1 Antenna Configuration with 1st ISB Substitution

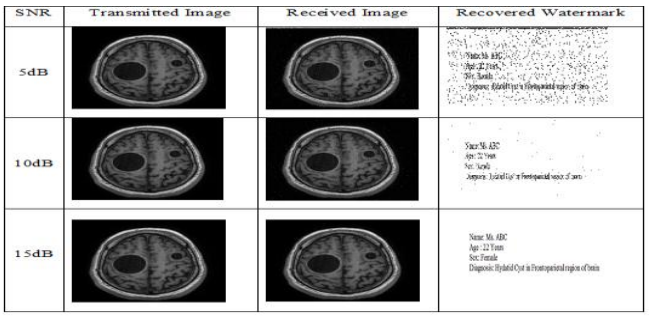

Fig 11: For 2×2 Antenna Configuration with 1st ISB Substitution

Thus with 1st ISB substitution the watermark is clearly visible at zero BER power levels of both the diversity order systems while as at other power levels the watermark has a noisy appearance. The readability of the watermark can thus be said to be power dependent for a given antenna configuration.

iii. Subjective analysis for case V and VI

The subjective quality results obtained case V and VI have been depicted in Fig. 12 and Fig. 13. The results clearly reveal that readability of the recovered watermark is increased as the SNR at the transmitter is increased from 20 to 30dB in case of 2×1 antenna configuration and from 5 to 15dB in case of 2×2 antenna configuration.

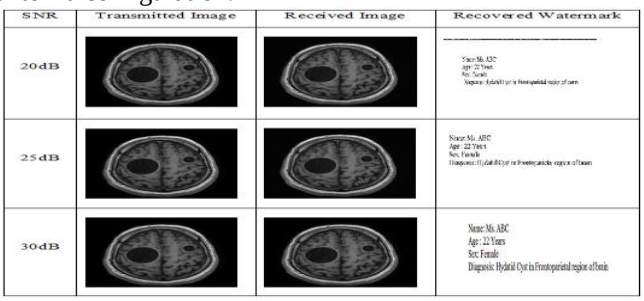

Fig 12: For 2×1 Antenna Configuration with 2nd ISB Substitution

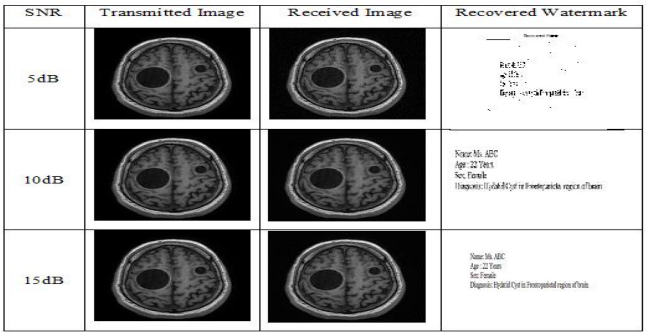

Fig 13: For 2×2 Antenna Configuration with 2nd ISB Substitution

Taking cognizance of all the above mentioned results (Fig 8 and 9, Fig 10 and 11, Fig 12 and 13) we conclude that the recovery of the watermark and its readability is a function of power and antenna configuration only and are independent of the embedding techniques used at the transmitter side. The visibility of the watermark gets enhanced as the power is increased from 15 dB to 30dB for 2×1 antenna and from 5dB to 15dB for 2×2 antenna for all the mentioned embedding schemes.

VII. CONCLUSION

In this paper a successful attempt to simulate and model a robust and secure wireless communication system for IoT driven e-health setup. MIMO-OFDM has been utilized because of its various advantages over the conventional single link communication systems. The working capability of the proposed system has been successfully demonstrated by transmitting a cover medical image with EPR embedded into it. Three different approaches of EPR embedding have been used-LSB embedding, 1st ISB embedding, 2nd ISB Embedding. It has been observed that ISB embedding deteriorates the quality of cover image more compared to LSB embedding, but is immune to LSB removal attack. All three schemes have been analysed under two different antenna diversity configurations (with fading environment conditions), resulting into six different cases. We have analysed all the six cases both subjectively and objectively and presented the results in the form of various Figures and Tables. Objective analysis has been carried out using various parameters like BER, PSNR, MSE, NCC and SSIM. QPSK modulation has been used during experimentation as it provides better trade-off between bandwidth utilization and BER. We have used ten most commonly used medical images to evaluate our scheme in terms of payload, imperceptivity and robustness. It has been seen that for a payload of 1bpp the average PSNR varies from 50.61dB in case of LSB embedding to 38.03dB for 2nd ISB embedding. This clearly shows that our scheme is able to provide better quality watermarked images, even in the worst case embedding. The watermarked image containing EPR has been transmitted over fading channels to test the robustness of the developed system against various channel attacks. It has been observed that the error rates decrease considerably with increase in SNR for a given antenna configuration. We have exploited antenna diversity to enhance the image reception and improve the readability of extracted watermark/EPR information. The observed results show that robustness is independent of embedding scheme but is direct function of antenna diversity and SNR. From the results it can be concluded that the proposed technique has lot of scope in e-healthcare system. The work presented can be extended to the next generation communication system with a minimal signal processing changes while as the underlying modulation and transmission techniques will remain the same. It is worth to mention that we have not considered Peak-to-Average Power-Ratio (PAPR) in this paper, which is a detrimental factor while designing any communication system. So the work presented in this paper could be further extended by integrating various PAPR reduction techniques. In addition the work presented in this paper assumes the perfect channel estimation and thus neglects all the estimation errors. We plan to observe the deteriorating effects on our framework by incorporating estimation errors, as a part of future work.

ACKNOWLEDGMENT

The authors would like to thank office of the Department of Science and Technology, Government of India, for supporting the work under the DST INSPIRE fellowship scheme.

REFERENCES

1. Parah, S. A., Sheikh, J. A., Ahad, F., Loan, N. A. and Bhat, G.M, "Information hiding in medical images: a robust medical image watermarking system for E-healthcare". Multimedia Tools Appl, DOI 10.1007/s11042-015-3127-y. 2005
2. Wang.D and Tureli.U, "Joint MIMO-OFDM and MAC Design for Broadband Multihop Ad Hoc Networks". EURASIP Journal on Wireless Communications and Networking, DOI 10.1155/WCN/2006/60585. 2006.
3. Zheng, Z. Sangaiah, AK., Wang. T. Adaptive Communication Protocols in Flying Ad Hoc Network, IEEE Communications Magazine 56 (1), 136-142.
4. Pan, S. Sun, W., Zheng, Z. Video segmentation algorithm based on superpixel link weight model, Multimedia Tools and Applications 76 (19), 19741-19760.
5. Zheng, Z., Zheng, Z.: Towards an improved heuristic genetic algorithm for static content delivery in cloud storage. Comput. Electr. Eng. (2017) https://doi.org/10.1016/j.compeleceng.2017.06.011.
6. Yao, S., Sangaiah, A.K., Zheng, Z., and Wang, T., Sparsity estimation matching pursuit algorithm based on restricted isometry property for signal reconstruction. Future Generation Computer Systems, 2017.
7. Shi, X. Zheng, Z. Zhou, Y. Jin, H. He, L. Liu, B. Hua, QS. Graph processing on GPUs: A survey, ACM Computing Surveys (CSUR) 50 (6), 81..
8. Starr J. C. T. And Silverman, P. "Understanding Digital Subscriber Line Technology". Prentice Hall, Upper Saddle River, NJ, USA. 1999.
9. Li, Y. and Stüber, Eds.G. "Orthogonal Frequency Division Multiplexing for Wireless Communications", Springer, New York, NY, USA. 2006.
10. Sheikh, J. A., Parah, S. A. and Bhat, G.M. "Orthogonal Variable Spreading Factor (OVSF) based image Transmission using Multiple Input Multiple Output Orthogonal Frequency Division Multiplexing (MIMO-OFDM) System". IEEE sponsored International Conference on Communications Devices and Intelligent systems" Jadavpur University, Kolkatta DOI 10.1109/CODIS.2012.6422132 pp 45-48 Print ISBN 978-1-4673-4699-3.2012
11. Balan, H. V., Rogalin, R., Michaloliakos, A., Psounis, K. and Caire, G. "AirSync: Enabling Distributed Multiuser MIMO with Full Spatial Multiplexing". IEEE/ACM Transactions, 2013.
12. Praveen, P., Likhitkar and Chandrasekhar, N. D. "Beamforming for MIMO-OFDM Wireless Systems". European Journal of Advances in Engineering and Technology, 2015, 2(6): 14-19. 2015

13. Osama W. Ata, Nemer A.M. Al-Amleh. "Application of MIMO Smart Antennas into WiMAX-OFDM System in Real Fading IEEE Standardized Channels". Proceedings of the World Congress on Engineering and Computer Science 2012 Vol II WCECS 2012, October San Francisco, USA. 24-26, 2012.
14. Akram M. Zeki and Azizah A. Manaf, "A Novel Digital Watermarking Technique Based on ISB (Intermediate Significant Bit)" World Academy of Science, Engineering and Technology 26 2009 .
15. Parah, SA. Akhoon, J. Loan, NA. Sheikh, JA. Bhat GM. Electronic Health Record hiding in Images for smart city applications: A computationally efficient and reversible information hiding technique for secure communication, Future Generation Computer Systems (2018), https://doi.org/10.1016/j.future.2018.02.023.
16. Ahad, F. Shabir, AP. Javaid, AS. Bhat, GM. Bhat Hiding clinical information in medical images: A new high capacity and reversible data hiding technique", Journal of Biomedical Informatics, DOI: http://dx.doi.org/10.1016/j.jbi.2017.01.006.
17. Muhammad, K. Sajjad, M. Mehmood, I., Rho, S. Baik, S. W. A novel magic LSB substitution method (M-LSB-SM) using multi-level encryption and achromatic component of an image," Multimedia Tools and Applications, 75(22), 14867-14893, 2016.
18. Chemak, C., Lapayre, J. C. and Bouhle, M. S. "New Watermarking Scheme for Security and Transmission of Medical Images for PocketNeuro Project". Radio Engineering, volume. 16, no. 4. 2007.
19. Korrai, P.K. "Performance analysis of different schemes for transmission of watermarked medical images over fading channels". M.Sc., Concordia University Montreal, Quebec, Canada. (2013).
20. Krishna, D., Anuradha, M.S. "Image Transmission through OFDM System under the Influence of AWGN Channel". International Conference on Advanced Material Technologies (ICAMT). (2016).
21. Parah, S.A. , Ahad, F., Sheikh, J.A., Loan, N.A. and Bhat G.M. "Pixel Repetition Technique: A High Capacity and Reversible Data Hiding Method for E-Healthcare Applications". In Intelligent Techniques in Signal Processing for Multimedia Security, Studies in Computational Intelligence .Springer International Publishing Switzerland . (2017).
22. Mishra, A., Sharma, K. and De, A "Quality Image Transmission through AWGN Channel using Polar Codes". International Journal of Computer Science and Telecommunications, volume 5, Issue 1. (2014).
23. Acharya, U. R, Bhat,S.P, Kumar,S. Min, C.L (2003). Transmission and storage of medical images with patient information. Computers in Biology and Medicine. Elsevier Volume 33, Issue 4, July 2003, Pages 303-310.
24. Parah, S.A. , Ahad, F., Sheikh, J.A., Loan, N.A. and Bhat G.M. "A New Reversible and high capacity data hiding technique for E-healthcare applications" Multimedia Tools Appl (2017) 76:3943–3975.
25. Abhilasha S, Malay KD (2014) "A blind and fragile watermarking scheme for tamper detection of medical images preserving ROI". IEEE International Conference on Medical Imaging, m- Health and Emerging Communication systems (MedCom).
26. Kamran AK, Sana AM (2014) "A high capacity reversible watermarking approach for authenticating images: Exploiting down-sampling, histogram processing, and block selection. Information Sciences". Elsevier. 256:162–183.
27. Loan N. A., Hurrah N. N. , Parah, S., Lee.J .W, Sheikh, J and Bhat G.M," Secure and Robust Digital Image Watermarking Using Coefficient Differencing and Chaotic Encryption" IEEE Access , Volume 6, 2018 DOI: 10.1109/ACCESS.2018.2808172.
28. Aparna P., Kishore P.V.V., "An Efficient Medical Image Watermarking Technique in E-healthcare Application Using Hybridization of Compression and Cryptography Algorithm". Journal of Intelligent Systems 27(1) · January 2017.
29. Muhammad, K., Ahmad. J, Rho S,. and Baik, W. (2017) "Image steganography for authenticity of visual contents in social networks". Multimedia Tools and Applications, pp.1-20.
30. Muhammad .K, M. Sajjad, I. Mehmood, S. Rho, and S. W. Baik, " Image steganography using uncorrelated color space and its application for security of visual contents in online social networks," Future Generation Computer Systems, 2, 2016, https://doi.org/10.1016/j.future.2016.11.029.
31. Potdar, V. , Han, S., & Chang, E. "A Survey of Digital Image Watermarking Techniques", 3rd International Conference on Industrial Informatics (INDIN 2005), pp709-716, 2005.
32. Sonia, Garg, N. K., Sing, G. "A Survey on Digital Image watermarking". International Journal of Advanced Research in Computer Engineering & Technology, volume 3, Issue 6. 2014.
33. Mona, M.E.G. "Comparison of two watermarking algorithms using DCT coefficients and LSB replacement". Journal of theoretical and applied Information Technology. 2008
34. K. Muhammad, J. Ahmad, N. U. Rehman, Z. Jan, and M. Sajjad, 2017. CISSKA-LSB: color image steganography using stego keydirected adaptive LSB substitution method. Multimedia Tools and Applications, 76(6), pp.8597-8626.
35. Siddiq, A. I. "Variable length cyclic prefix OFDM using Multipath delay tracking". Tikrit Journal of Engineering Sciences, volume 18, no. 2. 2011.
36. Akhoon, J. Parah, SA. Loan NA. Sheikh JA. Bhat, GM. Information hiding in edges: A high capacity information hiding technique using hybrid edge detection", Multimedia Tools and Applications, Springer, DOI: 10.1007/s11042-016-4253-x.
37. Dey, N. Shabir, P. Sheikh, J. Bhat GM. Realization of a new robust and secure watermarking technique using DC coefficient modification in pixel domain and chaotic encryption, Journal of Global Information Management., 26(4), 2017.
38. Parah, S. Sheikh, J. Bhat GM. Data hiding in color images: a high capacity data hiding technique for covert communication Computer Engineering and Intelligent Systems 4 (13), 107-115.

AUTHORS PROFILE

Uzma is a doctoral scholar in the Department of Electronics and IT, University of Kashmir and is currently working on the Performance Evaluation of MIMO-OFDM Systems and their Extended Applications. She is an INSPIRE fellow of Department of Science and Technology, Government of India**.**

Ghulam M. Bhat obtained his M.Sc. (Electronics) from the University of Kashmir, Srinagar (India) in 1987, M.Tech. (Electronics) from Aligarh Muslim University (AMU), Aligarh (India) in 1993 and Ph.D. Electronics Engg. from AMU, Aligarh, (India) in 1997. The major field of research of Dr. Bhat is Signal Processing Techniques and Secure Message Communication. He has served as Assistant Professor, Associate professor and now as Professor & Head, Department of Electronics and Instrumentation Technology, University of Kashmir. He has published many research papers on his area of interest. He has worked in the area of Mobile Radio Communication, Spread Spectrum Communication and Neural Networks and has guided many research degrees leading to the award of M.Phil and Ph.D. His present research interests include Secure Message communication, Neural networks and Signal Processing techniques for communication

Javaid A Sheikh has completed his M.Sc., M. Phil and Ph. D in Electronics from University of Kashmir, Srinagar in the year 2004, 2008 and 2012 respectively in the field of communications and Signal Processing. He is working as Assistant Professor in the department of Electronics and I. T University of Kashmir, Srinagar. His fields of interest are Wireless Communications, design and development of efficient MIMO OFDM based wireless communication techniques, Spread Spectrum modulation, Digital Signal Processing, Electromagnetics. He has published about sixty research papers in International and National journals and conference proceedings